A Low-Cost Fabrication Technique for Symmetrical and Asymmetrical Layer-by-Layer Photonic Crystals at Submillimeter-Wave Frequencies

Ramon Gonzalo, *Student Member, IEEE*, Beatriz Martinez, Chris M. Mann, Harm Pellemans, Peter Haring Bolivar, and Peter de Maagt, *Senior Member, IEEE*

***Abstract*—This paper presents a rapid, versatile, and practical technique for the manufacture of layer-by-layer photonic crystals in the millimeter- and submillimeter-wave regions. Mechanical machining is used to derive a rugged layer-by-layer structure from high-resistivity silicon wafers. Unlike traditional anisotropic etching techniques, this method does not rely on any particular crystal orientation of the substrate and allows greater flexibility in the photonic crystal design. Automatic alignment of alternating layers is achieved via careful placement of the separation cuts. Using this ability, two configurations of photonic crystals are realized and their RF characteristics are measured and presented. Firstly, a symmetrical photonic crystal is studied as an initial demonstration of the technique. This is followed by an asymmetrical example, where a different frequency response is observed for the two orthogonal polarization of the incident radiation. Two measurement techniques are used to characterize the photonic crystals and the merits of each are discussed. Theoretical predictions are seen to agree well with the measured behavior.**

***Index Terms*—Photonic crystal, planar antennas, submillimeter-wave antennas, surface-wave modes.**

I. Introduction

THE area of periodic electromagnetic materials is currently one of the most rapidly advancing sectors in electromagnetics. Periodic structures such as photonic crystals provide the ability to control the propagation of electromagnetic waves to an extent that was not previously possible [1] and, consequently, much effort is now being concentrated on their design and manufacture.

Since their discovery and first demonstration in the late 1980s [2], [3], interest in photonic crystals has grown explosively. From the literature, it is clear that the emphasis is placed more and more on finding tangible applications and carrying out detailed modeling rather than physical demonstration of the concept. Such is the potential for their use as highly efficient microwave devices, antennas, and optical lasers, that great excitement for this new multidisciplinary field of study has emerged.

Following the theoretical prediction of their existence, it was several years before a photonic crystal was finally physically demonstrated and its properties subsequently measured. This was mainly due to the practical difficulties associated with their manufacture. Eventually, a photonic crystal working at microwave frequencies was realized by Yablonovitch and his coworkers by mechanically drilling holes into a block of dielectric material. This material, i.e., "Yablonovite" [4], prevents the propagation of microwave radiation in any three-dimensional (3-D) spatial direction, although the material in its solid form is transparent at these wavelengths. Due to this ability to suppress unwanted radiation in three dimensions, 3-D photonic crystals have attracted much interest in the field of antennas. While two-dimensional photonic crystals have proven to make a useful substrate for planar antennas, a 3-D photonic crystal seems even more desirable because any antenna fundamentally radiates in three dimensions.

Many of the technological problems associated with photonic crystals are practical and usually relate to the mode of manufacture used. To this end, some ingenious methods to produce such 3-D crystals at microwave frequencies have recently been successfully developed. More or less simultaneously, Ho *et al.* [5] and Sozuer and Dowling [6] fabricated a photonic crystal with a bandgap at microwave wavelengths by stacking micromachined silicon wafers in a layer-by-layer or woodpile structure.

The layer-by-layer crystals reported in [7]–[9] are fabricated by means of etching silicon wafers and stacking the layers on top of each other. This simple one-step fabrication technique has been highly successful, but the resulting structures can be fragile. This is because the dielectric rods have a large aspect ratio and are supported only at their ends, making them susceptible to breakage. To tackle this problem, a double-sided etch approach was adopted in [10]. This comes at the cost of increased processing and restricts the dielectric rods on opposite faces of the wafer to an angle of 70.5° due to the anisotropic etching behavior.

Due to the associated fabrication problems, most photonic crystals have been demonstrated at microwave frequencies. As the physical size of a photonic crystal is governed by the effective wavelength of the radiation, the resulting photonic crystals at microwave frequencies can be quite bulky, limiting their practicality for commercial applications. New and

Manuscript received October 18, 2001. The work of H. Pellemans was supported in part by the European Union under the Training and Mobility of Researchers Interact Program.

R. Gonzalo and B. Martinez are with the Electrical and Electronic Department, Universidad Publica de Navarra, E-31006 Pamplona, Navarra, Spain.

C. M. Mann is with the Millimeter-Wave Group, Rutherford Appleton Laboratory, Oxfordshire OX11 OQX, U.K.

H. Pellemans and P. Haring Bolivar are with the Institut fuer Halbleitertechnik II, Rheinisch-Westfälische Technische Hochscule Aachen, 52056 Aachen, Germany.

P. de Maagt is with the Electromagnetics Division, European Space Research and Technology Centre, 2201 AG Noordwijk, The Netherlands.

Digital Object Identifier 10.1109/TMTT.2002.803446.

emerging applications such as medical imaging and secure high-bandwidth communication are driving the technology to ever shorter wavelengths. Their fabrication has been relatively difficult and their use correspondingly sparse, although some layer-by-layer structures have been fabricated and measured at infrared wavelengths [11]–[13]. The work presented in this paper describes a method for the fabrication and alignment of symmetrical and asymmetrical layer-by-layer crystals at submillimeter wavelengths. It has the advantage of ease and speed of manufacture, robustness, and design flexibility, thus offering the possibility for rapid prototyping. The manufacturing technique is based on the rather crude, but effective technique of direct machining both sides of a high-resistivity silicon wafer [14]. With the advancement of new deep dry-etch processing capability, the same concept could take advantage of the extra accuracy and geometric flexibility provided to realize otherwise unobtainable photonic crystal structures. An elegant automatic alignment procedure is described in detail. Symmetrical and asymmetrical layer-by-layers structures have been manufactured and their performance measured. Good agreement has been achieved between the theoretical and measured RF characteristics.

II. Design of the Layer-by-Layer Photonic Crystal

As stated in Section I, one possible implementation of a 3-D photonic crystal is the so-called woodpile or layer-by-layer structure [5], [6], [15]. The structure is made up of layers of silicon bars with each layer consisting of parallel bars having a normalized center-to-center separation of a (normalized value). The bars are rotated by 90° in each successive layer. Starting at any reference layer, the bars of every alternate layer are parallel to the reference layer, but shifted by a distance of $0.5a$ perpendicular to the bar axis. The stacking sequence is repeated every four layers (see Fig. 1). In this paper, the bars of different layers in the same stacking direction are at an angle of 60°. By using this configuration, a triangular–hexagonal structure of bars is obtained. The selection of 60° results in a center-to-center height between bars of the reference layer and the next layer with identical stacking of $\sqrt{3}a$. As the structure is formed by square bars touching each other, this total height is equal to four times the height of a single bar. This results in a bar height of $0.433a$.

Having fixed the basic geometry, it is possible to determine the structure's behavior. The method used for analysis was the well-known plane-wave analysis [16], [17]. This method starts with the Maxwell's equations in a generalized eigenvalue form. The plane-wave expansion allows this set of equations to be solved by converting them into a Hermitian eigenvalue problem. Using the appropriate unit cell vectors in the plane-wave analysis, the resulting dispersion relation as function of the irreducible Brillouin zone is shown in Fig. 2. A total of 32 000 plane waves were used in the calculations, which it is adequate for an accurate representation of the lowest modes. A complete gap has been obtained for a normalized frequency range from 0.285 to 0.316, representing a gap–midgap ratio of 10.3%. In the normal incidence case (point $E3$ in Fig. 2), the gap extends from 0.2388 to 0.316 (35.5% of gap–midgap ratio).

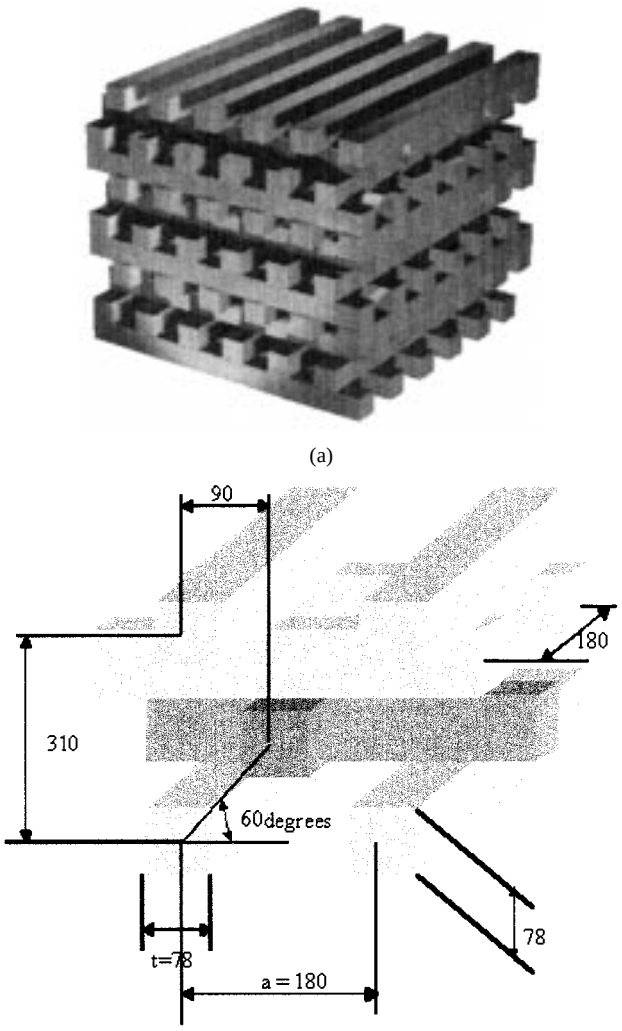

(a)

(b)

Fig. 1. (a) Schematic of the layer-by-layer photonic crystal structure. (b) Layer-by-layer dimensions (in micrometers) used.

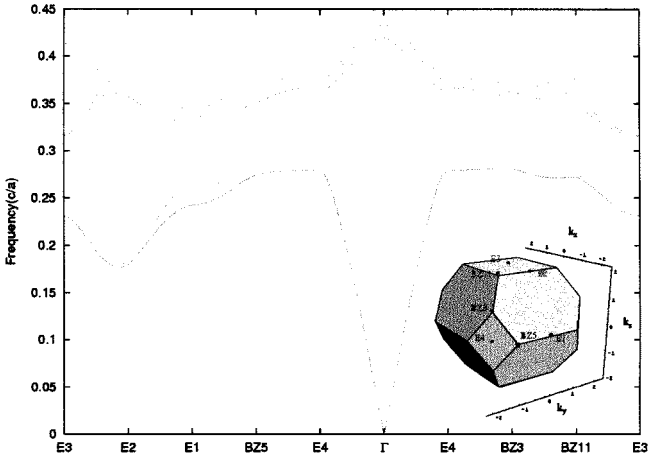

Fig. 2. Dispersion relation for the designed triangular–hexagonal layer-by-layer photonic crystal. The first Brillouin zone is shown in the inset.

A frequency of 500 GHz was selected for the demonstration of this technique, as it would put sufficiently stringent dimen-

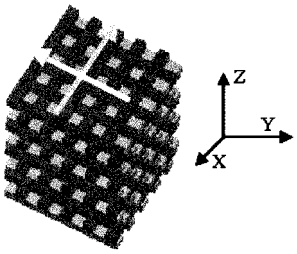

(a)

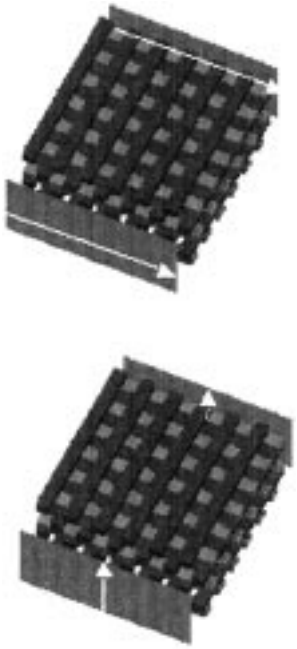

(b)

Fig. 3. Schematic of the layer-by-layer crystal structure used in the HFSS simulation to calculate the transmission parameters under: (a) normal and (b) lateral incidence. The different arrows represent the two different polarizations.

sional tolerancing on the fabrication and alignment process to test its suitability at submillimeter-wave frequencies.

By fixing $(fa/c) = 0.3$, which is close to the center of the gap for normal incidence, and $f = 500$ GHz, the physical values of $a = 180$ μm and bar thickness of $t = 78$ μm are obtained [see Fig. 1(b)]. These values lead to a frequency gap between 395–530 GHz for normal incidence. To verify and complement these results, the finite-element software Ansoft HFSS was used. By defining the input port to the topmost layer and the output port to the bottom of the layer-by-layer structure (normal incidence case), as indicated in Fig. 3, the transmission results can be obtained. The S_{21}-parameters for the two incident perpendicular polarizations (TE and TM) have been analyzed, and the results are shown in Fig. 4(a). The obtained results show that the two polarizations are degenerate, exhibiting the same S_{21}-parameter behavior, as it was expected from the symmetry of the structure in that direction of propagation.

The results in Fig. 4(a) should approximately coincide with the corresponding normal incidence propagation point E_3 in the dispersion relation in Fig. 2. In this point, the modes are degenerate. The gap edges ($-$10-dB point) extend from 380 to 525 GHz, not too dissimilar from the previous predicted

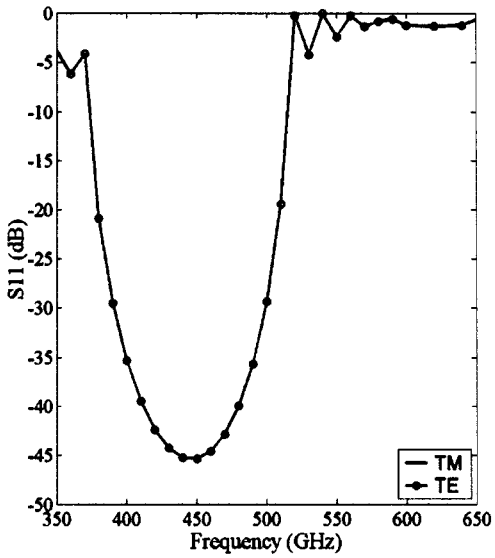

(a)

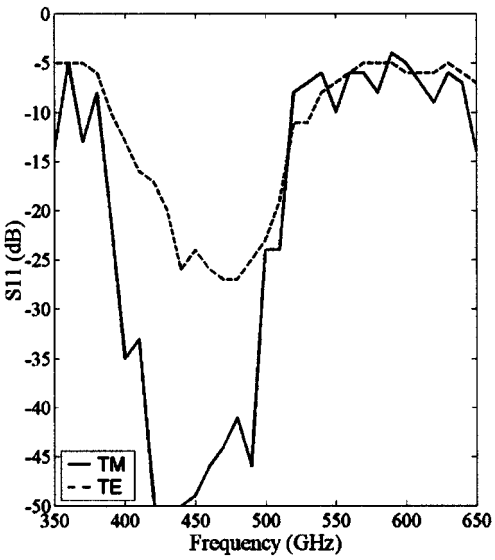

(b)

Fig. 4. S_{21}-parameter for the two orthogonal incident polarizations (TE and TM). (a) Normal incidence. (b) Lateral incidence.

results with the plane-wave analysis. The difference between the results can easily be explained based on the assumption in the plane-wave analysis that the crystal is infinite in size, while HFSS takes into account the finiteness.

The results for lateral incidence shown in Fig. 4(b) (using the appropriate input and output ports, see Fig. 3) present a different behavior as a function of the incident polarization. This is again in agreement with the plane-wave analysis, as lateral incidence corresponds to point $E1$ in Fig. 2.

III. Layer-by-Layer Fabrication Process

Once the layer-by-layer photonic crystal was theoretically analyzed, the fabrication process was carried out. While anisotropic wet etching of silicon [7]–[9] can be used with success for the formation of a channel with vertical walls, the process has its limitations, i.e., process control, alignment to

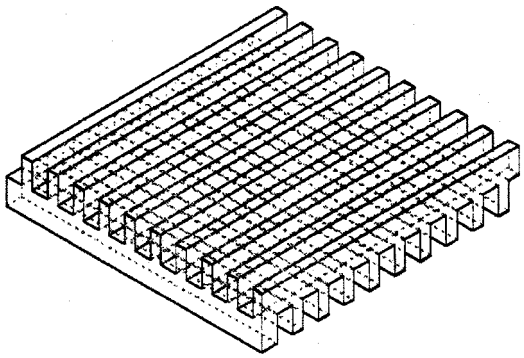

Fig. 5. Schematic of how the fabrication process is carried out. Two arrays of grooves are joined at the crossing point. This figure depicts half a period of the layer-by-layer structure.

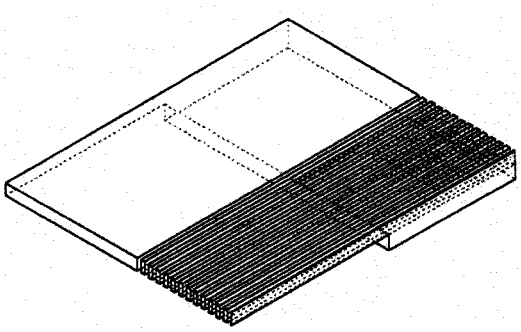

Fig. 6. Schematic showing the dicing of just one of the wafers faces.

crystal planes, sufficient aspect ratio, fabrication time, and limited structural integrity.

An alternative approach for the fabrication has been used [14]. This is based on the formation of such grid arrays by using mechanical dicing via the use of a high-speed diamond-cutting wheel of the sort used as a standard in the silicon industry. The resulting silicon structure has a series of grooves cut into both the front and back faces of the wafer. The depth of cut is set so as to open a window at the crossing point of the cuts, but leave the array joined at the crossing points of the resulting bars (see Fig. 5). This process has a number of advantages, namely, the manufacturing time, robustness, and the fact that the spacing and depth of the grooves can be set very accurately due to the ± 5-μm precision available. The smallest dimension that can be machined by the dicing saw used for this study is defined by the following values:

1) repetition spacing 60 μm;
2) bar thickness 30 μm;
3) maximum bar depth 200 μm.

This corresponds to a maximum operational frequency around 1.5 THz for a silicon-based photonic crystal.

The selected material for the fabrication was silicon (11.7 as the dielectric constant) with a resistivity greater/equal to 1000 $\Omega \cdot$ cm and a thickness of 155 ± 2 μm , as obtained from Virginia Semiconductor Inc., Fredericksburg, VA.

The high resistivity of the wafers was selected to minimize absorption loss in the silicon, as the loss tangent is directly proportional to the conductivity, which is inversely proportional to the resistivity. The selected thickness corresponds to half of the thickness periodicity, which contains two layers of bars. It was selected in this way in order to apply the fabrication process indicated previously (see Fig. 5).

The first step is to open up the grooves in one side of the wafer (see Fig. 6). The selected cutting depth was 80 μm (slightly more than half the total silicon thickness to ensure that the windows are opened). Before proceeding with the cutting of the backside, the square silicon wafer is fixed by using a thermal wax to a larger glass wafer. This step is used, as there is a danger that pressurized water used to remove debris passes through the windows opened in the photonic crystal. The water can otherwise lift the partly diced wafer from the tacky membrane used to secure it to the saw table. By incorporating this step, the water is prevented from getting under the photonic crystal by the wax. Use of a glass substrate allows inspection to ensure that there are no bubbles trapped in the underlying grooves.

When both sides of the wafer have been diced, half of a complete period of the layer-by-layer structure is obtained. The area of the layer-by-layer structure produced from a 75-mm-diameter wafer is approximately 25 cm^2. At 500 GHz, only a few square millimeters are required, thus, for practical purposes, it was decided to cut the wafer into 9-mm squares. These could then be stacked to generate the entire layer-by-layer structure. Each of the smaller pieces consisted of approximately 50 periods in the x–y-plane and half a period in the stacking direction (z).

Automatic alignment and $0.5a$ period offset of successive layers is achieved by cutting the segments of the layer-by-layer in a specific way (process depicted in Fig. 7). Successive bars in the z-axis were automatically aligned during the dicing process itself, i.e., the bars lie orthogonal to one another. To achieve the alignment in both x and y, simultaneously opposing corners of each segment were cut so that they were 1/2-period offset in both x and y. Thus, a simple fixture incorporating an accurately machined right-angle recess was used to align the layers. Each alternate layer was flipped through 180° with respect to the previous and pushed into the corner of the fixture. In this way the 1/2 period in x and y was maintained for successive 1/2 periods in z. By using this technique, the yield of the substrate material is optimized by minimizing wastage between cuts. It has been found that it is unnecessary to incorporate a supporting silicon frame because the individual bars are self supporting and, therefore, sufficiently robust to withstand subsequent manual handling.

After stacking all the pieces, the layer-by-layer photonic crystal was obtained (see Fig. 8). The final size was $9 \times 9 \times 1.55$ mm. The complete structure is obtained by fixing the individual layers with epoxy glue, which is liberally applied to their outermost edges.

IV. Measurements of the Symmetrical Layer-by-Layer Photonic Crystal

There are various techniques for determining the fabricated layer-by-layer crystal structure's RF properties around 500 GHz.

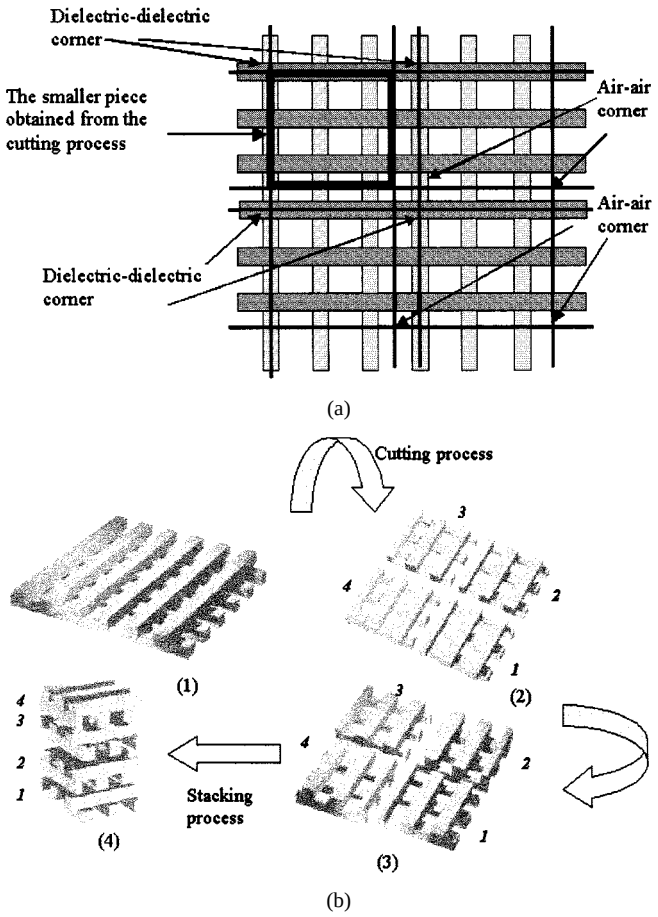

Fig. 7. Schematic of the cutting process used. (a) Top view of the process: each grey shade represents a different layer. Lines show the positions where the separation cuts are performed. (b) Representation of the whole process. From (2) to (3), the second and fourth pieces have been rotated 180°. (4) shows the final stacking configuration.

The method used to measure the transmission of the symmetrical layer-by-layer crystal structure is based on time-domain terahertz spectroscopy [14], [18], [19]. A schematic overview of the setup is shown in Fig. 9. A mode-locked Ti : sapphire laser produces optical pulses with a width of 100 fs and a repetition rate of 76 MHz. A beamsplitter is used to obtain two synchronized pulses of unequal intensity. The stronger pulse generates broad-band terahertz radiation from an InGaAs surface-field emitter. Parabolic mirrors collimate the terahertz beam, refocus it at the sample position, and image it onto the detector. The detector is a dipole antenna with an LT–GaAs ultrafast photoconductive sampling switch, and is gated by the weaker of the two optical pulses. Varying the relative delay time of the two optical pulses in the standard pump–probe method coherently measures the time-dependent electric field of the propagated pulse, and yields both amplitude and phase information. The complex transmission of the sample is determined by measuring the time-dependent terahertz signal with and without the sample. The setup provides a signal-to-noise level of approximately 40 dB around the bandgap frequency, with a usable bandwidth from 0.15 to 3.5 THz. Freestanding wire-grid polarizers were used to check that the terahertz radiation was linearly polarized. The experiment was carried out under a dry nitrogen atmosphere to suppress water vapor absorption.

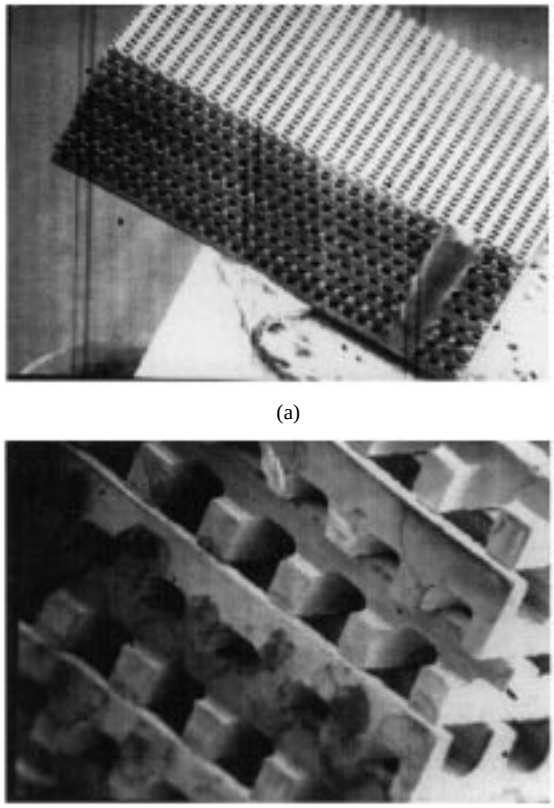

Fig. 8. Fabricated photonic crystal. (a) Fabricated layer by layer photonic crystal. (b) Detailed view.

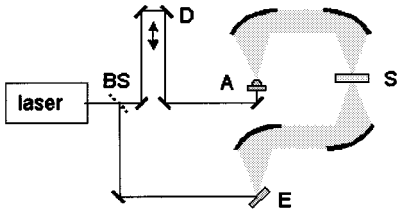

Fig. 9. Terahertz TDS setup, as used in the transmission experiments. BS: beam splitter. D: optical delay stage. E: InGaAs surface-field terahertz emitter. A: photoconductive terahertz detector. S: sample.

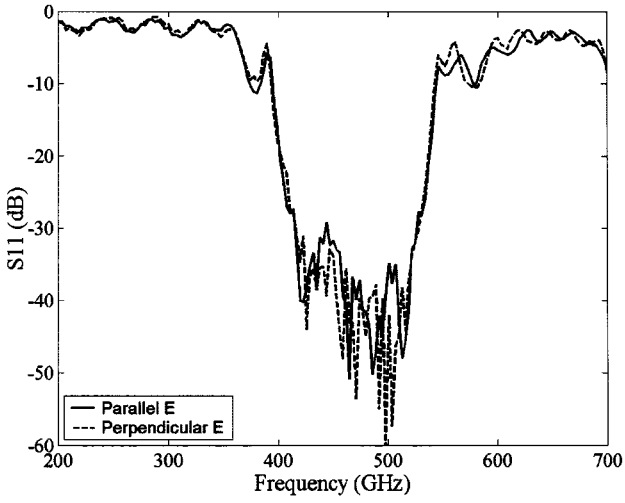

Fig. 10. Transmission results for normal incidence to the layer-by-layer crystal structure using the terahertz spectroscopy method.

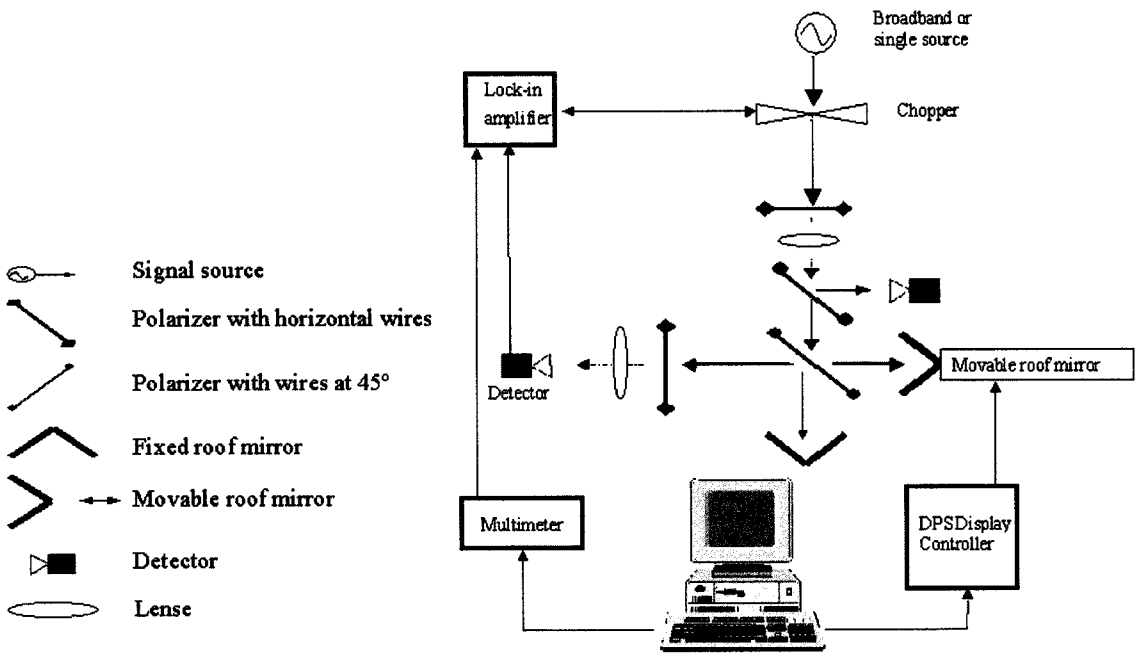

Fig. 11. Measurement setup.

The measured transmission as a function of frequency for the two possible photonic crystal orientations is shown in Fig. 10. The measured results for both polarizations coincide well with simulations and are of equal magnitude, indicating that the accuracy achieved with the fabrication technique was acceptable.

V. Measurements of the Asymmetrical Layer-by-Layer Photonic Crystal

Since the silicon is directly machined, the depth to which the grooves are made can be varied at will across the wafer. This allows the possibility to produce asymmetric structures where the material presents different physical dimensions to orthogonal polarizations. To our knowledge, this is something that has not yet been achieved using the anisotropic etching of silicon. To demonstrate this ability, a second photonic bandgap (PBG) layer-by-layer was fabricated where a polarization asymmetry was introduced into the crystal by adjusting relative depths of the silicon bars. This can be easily achieved by tilting the wafer slightly during dicing. Alternatively, more modern dicing saws have the ability to set the height of each individual cut via computer programming. The asymmetrical layer-by-layer structure has a bar height of 75 μm in one direction and 65 μm in the orthogonal direction.

It was shown earlier both theoretically and experimentally that the behavior of the layer-by-layer structure as a function of polarization should be identical for the symmetrical structure at normal incidence. For the asymmetrical structure, this is no longer the case, and the frequency response for parallel and perpendicular polarization is different.

The setup used for measurements on such an asymmetric structure was different from the one adopted for the symmetrical structure.

The terahertz time-domain spectroscopy (TDS) technique provides a fast method to measure the broad-band frequency response of the symmetrical photonic crystal. Terahertz–TDS systems have been demonstrated to be capable of measurements with high dynamic range [20], [21]. However, an increase in the signal-to-noise ratio above 40 dB requires either advanced modulation techniques or significantly longer measurement times. For the asymmetrical photonic crystal, it was important to be able to resolve the different behavior actually within the gap, where a high dynamic range is needed. In this instance, therefore, a coherent narrow-band tunable submillimeter-wave source was used, which is capable of a very high signal-to-noise ratio at a single frequency point. The higher signal-to-noise ratio of this source comes at the expense of measurement time, as the parallel acquisition of multiple frequencies, inherent to terahertz–TDS measurements, is lost. The narrow-band source was used in combination with a Fourier transform spectrometer to distinguish between its output harmonics.

The selected configuration for the Fourier transform spectrometer is based on a Martin–Puplett interferometer (MPI) [22]. This two-beam interferometer produces a variation in the detected output power as a function of the path difference between the two beams, which is provided in a controlled manner by computer control. The resulting data can then be Fourier transformed to obtain a measure of the signal power-frequency spectrum.

The MPI system used is illustrated in the central boxed part of Fig. 11. The incoming signal is split into two equal components, which are recombined after being directed along paths of different lengths. The resulting output signal is modified in a way that is related to the path difference and signal wavelength.

The detector was a hot electron bolometer (HEB) from QMC Instruments Ltd., Billinghurst, West Sussex, U.K. It had an electrical responsivity $>$5000 V/W, an electrical noise equivalent power (NEP) $< 5 \times 10^{-13}$ WHz$^{-1/2}$ and has a functional range from 60 GHz to 3 THz. The RF source was from ELVA-1 in the form of a 75–110-GHz backward-wave

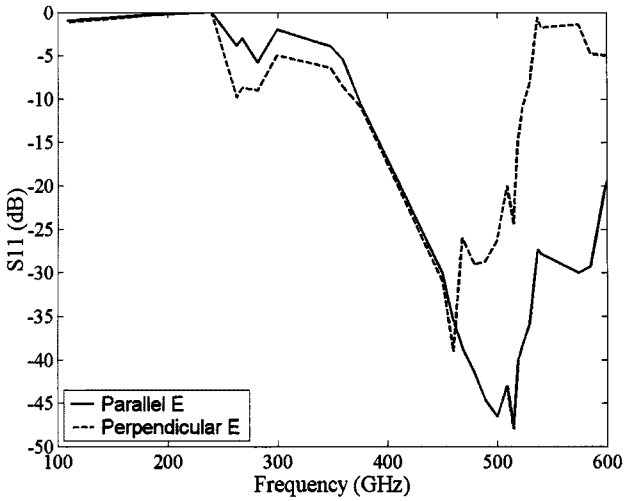

Fig. 12. Transmission results for normal incidence to the layer-by-layer crystal structure. The parallel and perpendicular orientations results are shown.

oscillator (BWO) driving a Rutherford Appleton Laboratory frequency multiplier. In order to cover all the desired measuring frequency range (300–600 GHz), different harmonics of the multiplier were used.

The complete setup used to measure the asymmetrical layer-by-layer photonic crystal features is depicted in Fig. 11. The MPI system is fed using the single-frequency chopped signal. A digital positioning system (DPS) controls the movement of the movable roof mirror and a lock-in amplifier retrieves the output power of the system. A computer controls the DPS and reads the output power from the lock-in amplifier. The data is recorded and Fourier transformed to obtain the frequency response of the entire system.

The asymmetrical layer-by-layer structure was placed either with the stacking direction parallel to the incident plane wave (parallel PBG) or perpendicular to the direction of the incident electric field (perpendicular PBG). By rotating the layer-by-layer crystal an angle of 90° on the measurement system, the parallel PBG configuration is converted into the perpendicular PBG configuration.

The measured insertion loss as function of frequency for each photonic crystal orientation is shown in Fig. 12. It should be noted that the acquisition of frequency points between 450–600 GHz were based on the fifth harmonic of the multiplier, while the third harmonic was used to obtain the lower frequency points. The rejection levels obtained at 500 GHz are better than −40 dB.

The performance of the asymmetrical structure was also theoretically predicted using HFSS. Fig. 13(a) shows the half-period of the layer-by-layer structure in which the asymmetrical bars have been included and Fig. 13(b) shows the transmission results for each one of the polarizations obtained. The measured results for both polarizations coincide well with simulations validating the fabrication method's ability to realize photonic crystal structures of sufficient mechanical tolerance.

The reason for the asymmetrical behavior of the crystal is that one polarization encounters bars of 75-μm height, and the other one of 65-μm height. This produces a shift in the transmission parameter S_{21} of one polarization in relation to the other. The

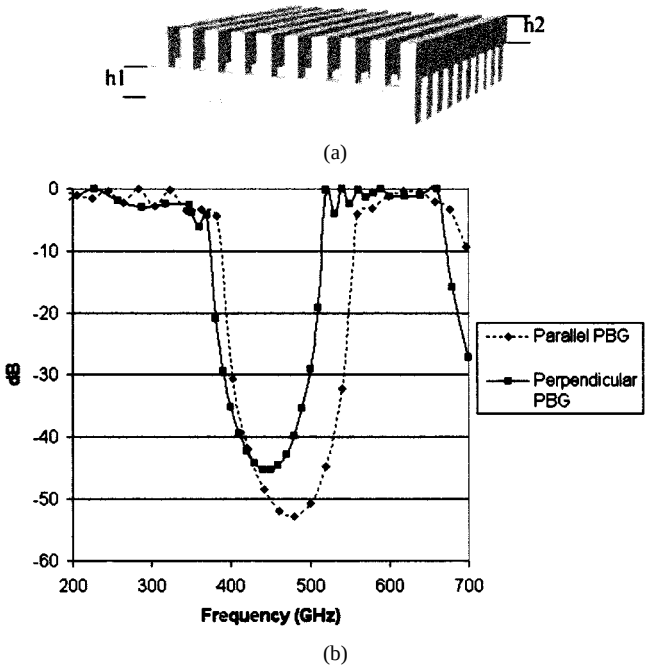

Fig. 13. (a) Schematic view of the fabricated error in the layer-by-layer photonic crystal structure. (b) Transmission parameters $S21$ of the layer-by-layer structure depicted in (a).

bars with lower height lead to a higher frequency response. Interesting to note is the fact that the isolation between to two polarizations reaches 27 dB for a corresponding insertion loss of only 0.6 dB at 540 GHz.

VI. Conclusion

A simple and versatile fabrication technique for the manufacture of submillimeter-wave photonic crystal has been described. The technique is easy to implement and produces a robust layer-by-layer structure. Total fabrication time is less than 6 h, 90% of which is either under automatic control or due to the curing schedule of the epoxy adhesive used. This technique should be able to provide sufficient dimensional accuracy to manufacture photonic crystals to approximately 1.5 THz. A corresponding elegant automatic alignment procedure has also been conceived.

Both symmetrical and asymmetrical layer-by-layer photonic crystal structures operating at 500 GHz have been designed, fabricated, and measured. Good agreement between simulations and measurements has been obtained.

For a four-layer symmetrical layer-by-layer photonic crystal structure, which has equal heights for orthogonal bars, there is no significant difference in performance for TE or TM polarized incident waves. If the bar heights are manufactured to be different for orthogonal directions, a significant dependence on the polarization of the incident wave has been determined.

The ability to introduce asymmetrical behavior in the crystal can be used in the future for devices whose properties will depend upon the field polarization. Therefore, this simple manufacturing and alignment technique represents a promising method for the rapid prototyping of millimeter-wave and submillimeter-wave photonic crystal structures.

ACKNOWLEDGMENT

The authors would like to thank the Millimeter-Wave Technology Group, Rutherford Appleton Laboratory, Oxfordshire, U.K., and Rheinisch-Westfälische Technische Hochscule Aachen (RWTH) Aachen, Aachen, Germany, for all the support in the fabrication and measurements.

REFERENCES

[1] J. D. Joannopoulos, R. D. Meade, and J. N. Winn, *Photonic Crystals: Molding the Flow of Light*. Princeton, NJ: Princeton Univ. Press, 1995.
[2] E. Yablonovitch, "Inhibited spontaneous emission in solid state physics and electronics," *Phy. Rev. Lett.*, vol. 58, pp. 2059–2062, 1987.
[3] S. John, "Strong localization of photons in certain disordered dielectric superlattices," *Phy. Rev. Lett.*, vol. 58, pp. 2486–2489, 1987.
[4] E. Yablonovitch, T. J. Gmitter, and K. M. Leung, "Photonic band structure: The face-centered-cubic case employing nonspherical atoms," *Phys. Rev. Lett.*, vol. 67, pp. 2295–2300, 1991.
[5] K. M. Ho, C. T. Chan, C. Soukoulis, R. Biswas, and M. Sigalas, "Photonic band gaps in three dimensions: New layer-by-layer periodic structure," *Solid State Commun.*, vol. 89, pp. 413–416, 1994.
[6] H. S. Sozuer and J. P. Dowling, "Photonic band calculations for woodpile structure," *J. Mod. Opt.*, vol. 41, pp. 231–234, 1994.
[7] E. Ozbay, E. Michel, G. Tutlle, R. Biswas, M. Sigalas, and K. M. Ho, "Micromachined millimeter-wave photonic band-gap crystals," *Appl. Phys. Lett.*, vol. 64, no. 16, pp. 2059–2061, Apr. 1994.
[8] E. Ozbay, A. Abeyta, G. Tutlle, M. Tringides, R. Biswas, C. T. Chan, C. M. Soukoulis, and K. M. Ho, "Measurement of a three-dimensional photonic band gap in a crystal structure made of dielectric rods," *Phys. Rev. B, Condens. Matter*, vol. 50, no. 3, pp. 1945–1948, July 1994.
[9] C. C. Cheng and A. Scherer, "Fabrication of photonic band-gap crystals," *J. Vac. Sci. Technol. B, Microelectron. Process. Phenom.*, vol. 13, no. 6, pp. 2696–2700, Nov./Dec. 1995.
[10] E. Ozbay, E. Michel, G. Tutlle, R. Biswas, K. M. Ho, J. Bostak, and D. M. Bloom, "Double-etch geometry for millimeter-wave photonic band crystals," *Appl. Phys. Lett.*, vol. 65, no. 13, pp. 1617–1619, Sept. 1994.
[11] J. G. Fleming and S. Y. Lin, "Three-dimensional photonic crystal with a stop band from 1.35 to 1.95 μm," *Opt. Lett.*, vol. 24, no. 1, pp. 59–51, Jan. 1999.
[12] S. Noda, N. Yamamoto, H. Kobayashi, M. Okano, and K. Tomoda, "Optical properties of three-dimensional photonic crystals based on III–V semiconductors at infrared to near-infrared wavelengths," *Appl. Phys. Lett.*, vol. 75, no. 7, pp. 905–907, Aug. 1999.
[13] S. Noda, K. Tomoda, N. Yamamoto, and A. Chutinan, "Full three-dimensional photonic crystals at near-infrared wavelengths," *Science*, vol. 289, no. 5479, pp. 604–606, July 2000.
[14] A. Chelnokov, S. Rowson, J.-M. Lourtioz, L. Duvillaret, and J.-L. Coutaz, "Terahertz characterization of mechanically machined 3D photonic crystal," *Electron. Lett.*, vol. 33, no. 23, pp. 1981–1983, Nov. 1997.
[15] E. Ozbay, E. Michel, G. Tuttle, R. Biswas, and K. M. Ho, "Terahertz spectroscopy of three-dimensional photonic band gap crystals," *Opt. Lett.*, vol. 19, no. 15, p. 1155, Aug. 1994.
[16] K. M. Ho, C. T. Chan, and C. M. Soukoulis, "Existence of photonic gap in periodic dielectric structures," *Phys. Rev. Lett.*, vol. 65, no. 25, pp. 3152–3155, Dec. 1990.
[17] H. S. Sozuer and J. W. Haus, "Photonic bands: Convergence problems with the plane-wave method," *Phys. Rev. B, Condens. Matter*, vol. 45, no. 24, pp. 13962–13 972, June 1992.
[18] C. Fattinger and D. Grischkowsky, "Terahertz beams," *Appl. Phys. Lett.*, vol. 54, pp. 490–492, 1989.
[19] M. C. Nuss and J. Orenstein, "Terahertz time-domain spectroscopy," in *Millimeter and Submillimeter Wave Spectroscopy of Solids*, G. Gruner, Ed. Berlin, Germany: Springer-Verlag, 1998.
[20] M. Brucherseifer, H. P. M. Pellemans, P. Haring Bolivar, and H. Kurz, "THz spectroscopy with ultrahigh sensitivity," in *Laser and Electro-Opt. Conf. Tech. Dig.*, San Francisco, CA, May 7–12, 2000, pp. 553–554.
[21] Z. Jiang, M. Li, and X.-C. Zhang, "Dielectric constant measurement of thin films by differential time-domain spectroscopy," *Appl. Phys. Lett.*, vol. 76, no. 22, pp. 3221–3223, May 2000.
[22] J. Lesurf, *Millimeter-Wave Optics, Devices and Systems*. Bristol, U.K.: Adam Hilger, 1990.

Ramon Gonzalo (S'95) was born in Logroño, La Rioja, Spain, on July 15, 1972. He received the M.Sc. (with honors) and Ph.D. degrees from the Public University of Navarra (UPNa), Navarra, Spain, in 1995 and 2000, respectively, both in ingeniero de telecomunicación.

Since October 1995, he has been with the Antenna Group, Electrical and Electronic Engineering Department, UPNa, where he is currently an Associate Professor. From September 1997 to December 1998, he was with the Antenna Section, European Space Agency–European Space Research and Technology Centre (ESA–ESTEC), where he was a Research Fellow, involved in the modeling and design of electromagnetic crystal devices at microwave and millimeter-wave frequencies. His current area of research includes the design of passive and active photonic band components for microwave and millimeter-wave applications with emphasis on antenna applications, design of waveguide transmission lines, and corrugated horn antennas.

Beatriz Martinez was born in Tulebras, Navarra, Spain, on October 29, 1973. She received the M.Sc. degree in ingeniero de telecomunicación from the Public University of Navarra (UPNa), Navarra, Spain, in 1997.

Since October 1997, she has been with the Antenna Group, Electrical and Electronic Engineering Department, UPNa, where she is currently a Research Assistant. From June 1999 to January 2000, she was with the Payload, Equipment, and Technology Section, Payload Systems Division, European Space Agency–European Space Research and Technology Centre (ESA–ESTEC), under a Spanish grant, where she was involved in the development of software tools for waveguide filters at microwave and millimeter-wave frequencies. Her current areas of research are in the field of electromagnetic band structures for microwave and millimeter-wave antenna applications with emphasis on space antenna applications, design of waveguide transmission lines, and development of software tools.

Chris M. Mann was born in London, U.K., in 1962. He received the B.Sc. degree (with honors) from Coventry Poletechnic, Lanchester, U.K., in 1985, and the Ph.D. degree from the University of London, London, U.K., in 1992.

From 1985 to 1992, he was an Associate Researcher with the Rutherford Appleton Laboratory (RAL), Oxfordshire, U.K., where he was involved with numerous aspects of millimeter-wave technology. In 1992, he joined the Photodynamics Research Centre, Sendai, Japan, where he was involved with the design of terahertz mixers. In 1994, he returned to RAL, where he played a leading role in the design, fabrication, and testing of terahertz waveguide mixers in 1995. Since then, he has continued this work, but is also involved with the optimization of submillimeter-wave frequency multipliers and subharmonic mixers. He also currently pioneers waveguide micromachining techniques in order to realize completely integrated submillimeter-wave RF frontends. For the past two years, he has held the part-time position of Chief Engineer with Flann Microwave Ltd, Bodmin, U.K.

Harm Pellemans, photograph and biography not available at time of publication.

Peter Haring Bolivar was born in Mexico City, Mexico, in 1969. He studied electrical engineering at the Rheinisch-Westfälische Technische Hochscule (RWTH) Aachen, Aachen University, Aachen, Germany, from 1987 to 1992.

During his thesis research, he made the first observation of Bloch oscillations, a fundamental phenomenon predicted since the beginnings of the 20th century. From 1992 to 1993, he was Head of the Rescue Equipment Division, Nautica Diesel Europea, Mexico City, Mexico. From 1993 to 1996, he was a Scientific Assistant with the Institut für Halbleitertechnik II, RWTH Aachen, where he was involved with conjugated polymers and femtosecond dynamics in semicoductors. From 1997 to 2001, he was Head of ultrahigh-frequency research with the Institut of Semiconductor Electronics, RWTH Aachen, where he directed applied and fundamental scientific research on coherent terahertz spectroscopy and ultrahigh-frequency optical characterization of electronic gigahertz devices. Since 2001 he has been Head of research at the RWTH Aachen, with ample activities in the fields of optoelectronics, ultrafast science, ultrahigh-frequency devices, optical data storage, and nanotechnology. He has authored or coauthored over 100 publications and international conference presentations and four book contributions. He holds two patents.

Dr. Haring Bolivar was the recipient of a Heinrich Hertz Fellowship from the Science and Research Ministry of the State of Northrhine–Westfalia and the Wilhelm Borchers Medallion of the RWTH Aachen.

Peter de Maagt (S'88–M'88–SM'02) was born in Pauluspolder, The Netherlands, in 1964. He received the M.Sc. and Ph.D. degrees from the Eindhoven University of Technology, Eindhoven, The Netherlands, in 1988 and 1992, respectively, both in electrical engineering.

He is currently with the European Space Agency–European Space Research and Technology Centre (ESA–ESTEC), Noordwijk, The Netherlands. His research interests are in the area of millimeter- and submillimeter-wave reflector and planar integrated antennas, quasi-optics, photonic-bandgap antennas, and millimeter- and submillimeter-wave components.

Dr. de Maagt was the co-recipient of the 2002 H. A. Wheeler Award presented by the IEEE Antennas and Propagation Society (IEEE AP-S) for the best applications paper of 2001.